http://journal.uir.ac.id/index.php/JGEET

E-ISSN : 2541-5794
P-ISSN : 2503-216X

Journal of Geoscience, Engineering, Environment, and Technology
Vol 10 No 4 2025

RESEARCH ARTICLE

Mineralogy and Geochemistry of Rare Earth Elements in Manganese Deposits in the Anabanua District, Barru Regency, South Sulawesi Province, Indonesia

Muhamad Hardin Wakila[1,*], Citra Aulian Chalik[1], Alam Budiman Thamsi[1], Nurliah Jafar[1], Harwan[1], Emi Prasetyawati Umar[1,2]

[1]*Department of Mining Engineering, Universitas Muslim Indonesia, Makassar, Indonesia.*
[2]*Department of Geological Engineering, Universitas Gadjah Mada, Yogyakarta, Indonesia.*

* Corresponding author : wakilahardin@umi.ac.id
Tel.:+62-852-55636440
Received: Sep 6, 2025; Accepted: Dec 19, 2025.
DOI: 10.25299/jgeet.2025.10.4.24882

Abstract

Research programmes on rare earth elements have not been widely carried out, especially on manganese deposits, even though manganese deposits also contain rare earth elements. Research on manganese mineralogy has been done before, however, research has not focused on rare earth metal elements found in manganese deposits, so further research is needed to find out the mineralogy, geochemistry, and gardes of rare earth metal elements in manganese deposits in the tropics. There are 3 methods of analysis at once, namely petrographic, XRD, and ICP-OES methods. The minerals found in manganese samples in the study area are: Albite, Chlorite, Plagioclase, Orthoclase, Quartz, Chlorite, Opaque, Pyrolusite, Muscovite, Diopside, Hematite, Rodochroite, Manganochromite and Manganite. Rare earth element levels in manganese deposits are Yttrium (8.7-35.5 ppm), Scandium (4-28 ppm), Lanthanum (5.3-122 ppm), Cerium (9.4-198 ppm), Praseodymium (1.3-23.6 ppm), Neodymium (690.9), Samarium (1.2-15. 4 ppm), Europium (0.6-3.5 ppm), Gadolinium (1.4-13.5 ppm), Terbium (0.241.75 ppm), Dysprosium (1.4-7.9 ppm), Holmium (0. 3-1.3 ppm), Erbium (0.8-3.2 ppm), Thulium (0.1-0.4 ppm), Ytterbium (0.8-2.4 ppm) and Lutetium (0.14-0.39 ppm). These results indicate that manganese deposits in Anabanua Village, Barru Regency, have the potential to be a source of LREE (La, Ce, Pr, Nd, and Sm) with concentrations exceeding those of several deposits around the world, making them worthy of consideration in strategic mineral exploration in Indonesia in general.

Keywords: Rare Earth Element, manganese, Petrographic, XRD, and ICP-OES.

1. Introduction

1.1 Sub Introduction

Rare earth elements as the name indicates are elements that are very rare or very few in nature in the form of complex compounds, generally phosphate and carbonate compounds. Along with the development of material processing technology rare earth elements are increasingly needed and generally in high-tech industries (Purawiardi, 2001). Indonesia has considerable potential for rare earth elements, but their exploration and exploitation have not been a priority. As a result, the development of this commodity has been insignificant in terms of global competitiveness. According to Burton (2022), rare earth metals are one of the important minerals increasing as the transition towards green energy growth demands. The term 'rare' in rare earth metals refers to their 'uncommon' presence due to their limited quantities and binding as complex compounds. Although under natural conditions, the abundance of these elements is actually widespread in the continental crust and is relatively easy to reach (Atwood, 2013). The REEs have a variety of applications in modern technology and provide many vital materials related to industry (Humphries, 2011). These elements are classified into light REEs (LREEs) including Ce, Eu, La, Nd, Pr, Sm, and Pm and heavy REEs (HREEs) consisting of Tm, Dy, Er, Gd, Ho, Lu, Tb, Yb, Sc, and Y (Jha, 2014; Simandl, 2014; Emsbo et al., 2015).

The presence of rare earth elements (REE) has been found in several commodities, one of which is manganese deposits. According to Miroyama et al in 2008, there is a high potential of rare earth metals, especially Heavy Rare Earth Elements (HREE) in manganese minerals that form stratiform in India caused by hydrothermal processes (Moriyama et al., 2008). Other research has shown the presence of rare earth elements in the Nikopol manganese deposit located west and north of Nikopol, Ukraine and is one of the world's largest deposits among sedimentary manganese deposits, with total REE content between 60 and 197 ppm, with an average of 108 ppm (Sasmaz et al., 2020).

Barru Regency is one of the areas in South Sulawesi that has unique geological conditions with various types of minerals, one of them is manganese deposits (Ariansyah et al., 2020). Research related to manganese deposits in Barru Regency has been conducted previously by Falah in 2009, namely a study of the presence of manganese in Patappa Village, Barru Regency. Then research on manganese mineralogy in the Palluda Region carried out by Sufriadin, et al in 2015; However, these studies did not focus on examining in detail the rare earth elements contained in manganese deposits, while Barru Regency has abundant manganese

resources. Therefore, further research is needed to determine the mineralogy, geochemistry, and content of rare earth elements in manganese deposits in tropical regions in general, especially in Anabanua Village, Barru District, Barru Regency, South Sulawesi Province.

1.2 Study Area

The study area is located in Anabanua District, Barru Regency, South Sulawesi Province, Indonesia, with coordinates 4^0 28" 22" S and 119^0 42" 45" E. This area has an area of 20 square kilometres. The study area is about 125 km from Makassar City (the capital of South Sulawesi Province) (Fig.1).

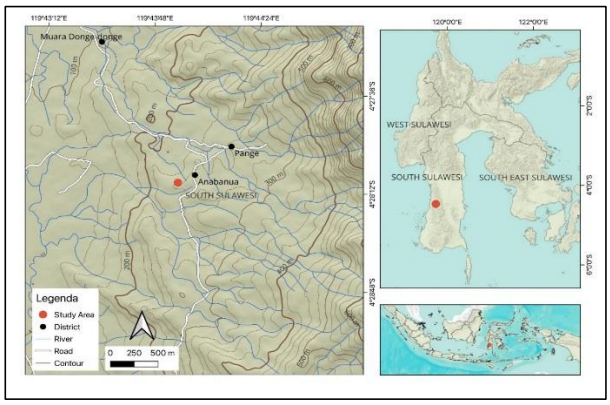

Fig. 1. Map of the research area.

2. Sample Collection and Analyses

This research starts by conducting a literature study on books and journals with similar studies to the object of research, then conducts field investigations to make observations and take manganese samples directly in the research area. There are 3 manganese samples taken from the results of field activities. The next stage is to conduct Petrographic analysis to determine the mineral content of manganese samples in the study area. Petrographic properties could only be observed or measured in thin sections (Ghobadi et al., 2015). Then further X-Ray Diffraction (XRD) analysis is carried out to determine the content of compounds that make up the manganese sample. X-Ray Diffraction analysis was performed on powdered rock reference samples to determine the mineralogical composition (Ranjbaran et al., 2019). The next stage is to conduct ICP-OES analysis to determine the content of rare earth elements contained in manganese samples in the study area. The use of the ICP-OES method has proven effective in identifying rare earth element content in rock samples (Yazdi et al., 2023). Petrographic, XRD, and ICP-OES methods were selected in this study because these three methods can provide comprehensive understanding: from microscopic (structure & texture), mineralogy (crystalline phase), to geochemistry (element content). The laboratory used to analyze petrography, XRD, and ICP-OES is the Laboratory at the Department of Geological Engineering, Hasanuddin University, Makassar, Indonesia.

3. Results

3.1. Petrographic Analysis

a. Sample 1

Petrographic analyses were carried out to identify mineral textures microscopically (Ahmed et al., 2023). In addition, detailed petrographic laboratory experiments, such as photomicrographs of thin sections and modal analyses, of each sample were conducted (Kupolati et al., 2020). The microscopic appearance of this rock incision has an absorbance colour of greyish brown, blackish grey interference colour, subhedral-anhedral shape, refractive index Nmin > Ncb. This rock has undergone alteration of about 70% of the mineral size 0.025 mm - 3 mm, with the alteration mineral being Albite-Chlorite. Figure 2 shows the presence of Plagioclase mineral with a percentage of (50%). The parallel nicol is transparent-light brown colour, subhedral prismatic shape, low relief, weak intensity, mineral size 0.5-3 mm, weak bicyclic pleochroism, 1-way cleavage (Fig. 2a). In the cross nicol, the presence of Orthoclase minerals with a percentage (30%), prismatic shape, medium relief, mineral size 0.3-2 mm, monochroic pleochroism, cleavage is absent, has a grey colour, yellow absorption colour, reddish brown interference colour, subhedral-anhedral shape, mineral size 0.025-0.8 mm, medium relief, medium intensity, does not have pleochroism (Fig. 2b). In both niches there is also the presence of opaque minerals with a percentage of (35%) In the appearance of parallel nicol this mineral has a black colour, euhedral-subhedral shape, mineral size 0.1-2 mm, and is isotropic.

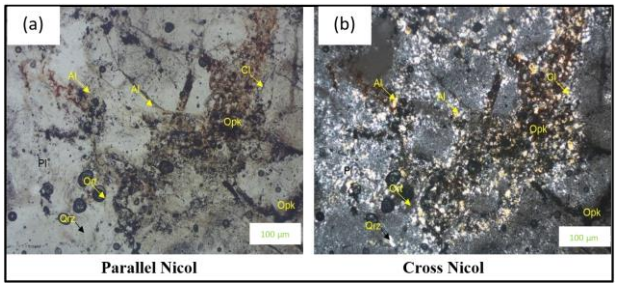

Fig. 2. Microscope view of sample 1

b. Sample 2

*t*he microscopic appearance of this rock incision has a greyish brown absorption colour, blackish grey interference colour, subhedral-anhedral shape, refractive index Nmin > Ncb. This rock has undergone alteration of about 70% with a mineral size of 0.025 mm-3 mm, with the alteration mineral being Albite-Chlorite.

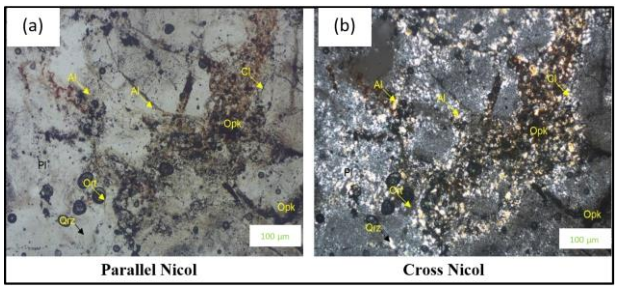

Fig. 3. Microscope view of sample 2

Figure 3 shows the presence of Plagioclase mineral with a high percentage (50%) in the parallel Nicol appearance. This mineral has a transparent-light brown colour, subhedral prismatic shape, low relief, weak intensity, mineral size 0.5-3 mm, 1-way split, grey in colour (Fig. 3a). In the cross nicol appearance, the presence of Orthoclase minerals with a percentage of (30%) is found, having a prismatic shape, medium insity, has no pleochrism. The last mineral encountered in the microscope observation of sample 2 is the Opaque mineral in the nicol alignment of this mineral with

black colour, euhedral-subhedral shape, mineral size 0.1-2 mm, isotropic (Fig. 3b).

c. Sample 3

The microscopic appearance of this rock has a greyish brown absorption colour, blackish grey interference colour, subhedral-anhedral shape, refractive index Nmin > Ncb. This rock has been altered by about 70% of the mineral size of 0.025 mm-3 mm, with the alteration mineral being Albite-Chlorite

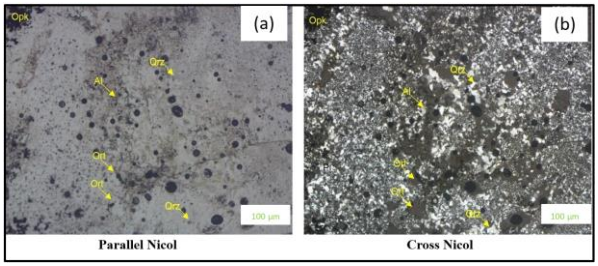

Fig. 4. Microscope view of sample 3

Figure 4 shows the presence of Plagioclase mineral with a percentage of (50%) in the parallel nicol appearance. This mineral is transparent-light brown, subhedral prismatic shape, low relief, weak intensity, mineral size 0.5-3 mm, 1-way split, grey in colour (Fig. 4a). In the cross nicol appearance, the presence of orthoclase minerals with a percentage of (30%), prismatic shape, medium relief, mineral size 0.3-2 mm, monochroic pleochroism, no cleavage, grey in colour. This observation also shows the presence of quartz mineral with a percentage of (20%), granular shape, low relief, weak intensity, monochroic pleocryism, mineral size 0.02-0.05 mm (Fig. 4b).

In the microscope view of sample 3, there is also the presence of albite mineral (5%), yellow absorption colour, reddish brown interference colour, subhedral-anhedral shape, mineral size 0.025-0.8 mm, medium relief, medium intensity, no pleocrism. And also found the presence of opaque minerals with a percentage of (35%) In the appearance of nicol aligned this mineral is black in colour, euhedral-subhedral shape, mineral size 0.1-2 mm, isotropic.

3.2 XRD Analysis

X-Ray Diffraction (XRD) analysis is a technique to identify the crystalline phase in materials, the crystalline form of the material varies in each material including minerals so that it is used as a characterisation of a mineral. XRD can display the mineral content and percentage of minerals from a sample (Mustafa et al., 2023). The measurement results acquired in the form of intensity per step (time step) by calculating time series statistical analysis. The measurement results per step are converted into a graph of intensity peaks which is also called a diffractogram (Karlinasari et al., 2023).

1. Sample 1

Based on the XRD (X-Ray Diffraction) results for sample 1, the presence of the minerals Quartz (SiO_2), Pyrolusite (MnO_2), Muscovite ($KaI_2(AlSi_3O_{10})(F,OH)_2$), Rhodochrosite ($MnCO_3$), and Manganite ($MnO_4$) were found. The following figure 5 is the appearance of the diffractogram graph of sample 1.

2. Sample 2

Based on the XRD results of sample 2, the presence of the minerals Manganochromite ($MnCr_2O_4$), pyrolusite (MnO_2), Quartz (SiO_2), Manganite (MnO_4), and Hematite (Fe_2O_3) were found. The following is a graph of XRD (X-Ray Diffraction) results for sample 2 in figure 6.

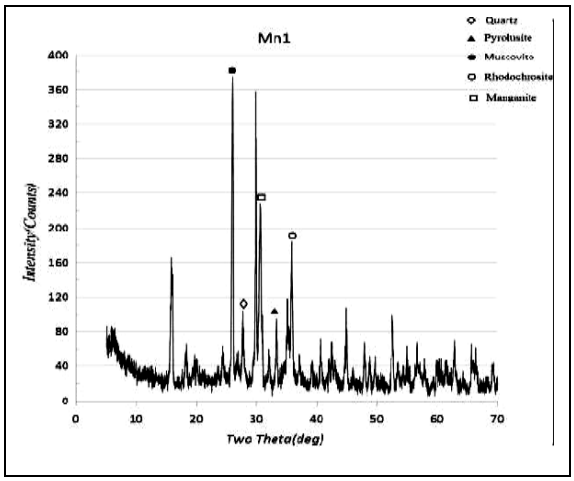

Fig.5. Difractogram of sample 1

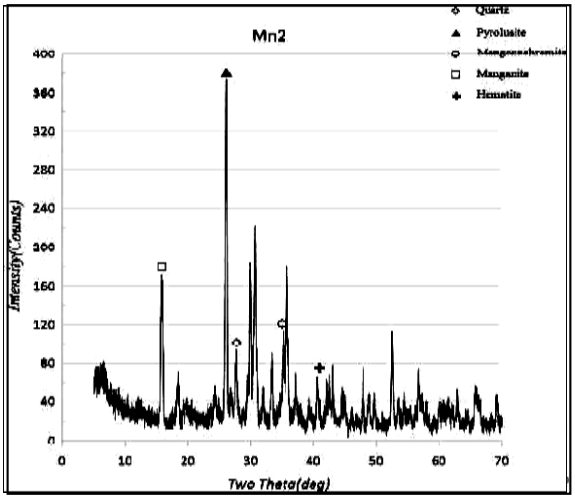

Fig.6. Difractogram of sample 2

3. Sample 3

Based on the XRD (X-Ray Diffraction) results of sample 3, the presence of the minerals Muscovite ($KaI_2(AlSi_3O_{10})(F,OH)_2$), pyrolusite ($MnO_2$), Quartz ($SiO_2$), Manganite ($MnO_4$), Hematite ($Fe_2O_3$), and diopside ($Si_2O_6$) were found. The following is a graph of XRD (X-Ray Diffraction) results for sample 3:

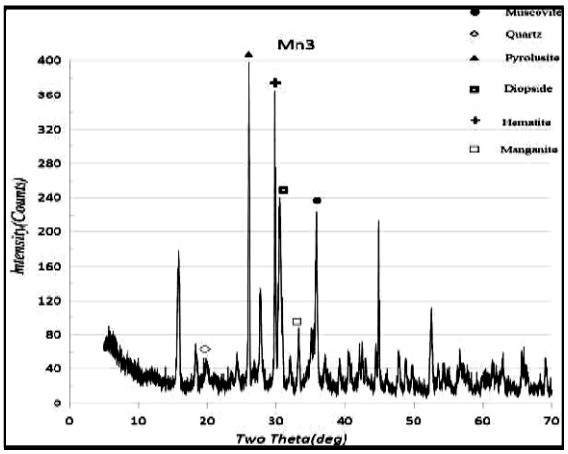

Fig. 7. Difractogram of sample 3

For better observation, a summary of all minerals from the results of Petrographic and XRD analyses can be seen in the following table (Table 1)

Table 1. Mineral summary of petrographic and XRD analysis results

No	Sample	Petrographic	XRD
1	Sample 1	Albite, Chlorite, Plagioclase, Orthoclase, and opaque	Quartz, Pyrolusite, Muscovite, Rhodochrosite, and Manganite
2	Sample 2	Albite, Chlorite, Plagioclase, Orthoclase, Quartz, chlorite, and Opaque	Manganocromite, pyrolusite, Quartz, Manganite, and Hematite
3	Sample 3	Albite, Chlorite, Plagioclase, Orthoclase, Quartz, and opaque	Muscovite, pyrolusite, Quartz, Manganite, Hematite, and diopside

3.3 ICP-OES Analysis

ICP is widely used for metal analysis in soil, sediment, and water. This tool can simultaneously measure analytes with high sensitivity and provide a low analyte detection limit to ppb units (Duz et al., 2016; Ilieva et al., 2018; Voica et al., 2012). ICP technique is used for the whole rock geochemistry (Al-Jubury et al., 2023). While ICP-MS offers high sensitivity and precision, but it is an expensive technique that demands stringent environmental conditions and a high level of technical expertise of operators (Qiao et al., 2022). Inductively Coupled Plasma Optical Emission Spectrometry (ICP-OES) has been widely applied in the analysis of surface water, mineral water, groundwater, brine and other samples (Ashok et al. 2023; Chen, 2016; Zou et al. 2017; Liu et al. 2022; Farhadiyan et al. 2024). ICP analysis was carried out on 3 manganese samples in the study area. Sample analysis results can be seen in the following table.

Table 2. ICP-OES analysis results

No	*Metal Elements*	*Sample 1 (ppm)*	*Sample 2 (ppm)*	*Sample 3 (ppm)*
1	Yttrium (Y)	35.5	8.7	27.6
2	Scandium (Sc)	28	4	9
3	Lanthanum (La)	122	5.3	23.2
4	Cerium (Ce)	198	9.4	34.2
5	Praseodymium (Pr)	23.6	1.3	5.49
6	Neodymium (Nd)	90.9	6	23.1
7	Samarium (Sm)	15.4	1.2	4.8
8	Europium (Elu)	3.5	0.6	1
9	Gadolinium (Gd)	13.5	1.4	4.6
10	Terbium (Tb)	1.74	0.24	0.75
11	Dysprosium (Dy)	7.9	1.4	4.7
12	Holmium (Ho)	1.3	0.3	0.9
13	Erbium (Er)	3.2	0.8	2.6
14	Thulium (Tm)	0.4	0.1	0.3
15	Ytterbium (Yb)	2.4	0.8	2.1
16	Lutetium (Lu)	0.39	0.14	0.34

Based on Table 1, it can be seen that the element that has the highest grade in sample 1 is the element Cerium (Cel) with a grade of 198 ppm, while the element that has the lowest grade is Lutetium (Lu) with a grade of 0.39 ppm. For sample 2 the element that has the highest grade is Cerium (Cel) with a grade of 9.4 ppm, while the lowest grade is the Thulium (Tm) element with a grade of 0.1 ppm. For sample 3, the element that has the highest grade is the element Cerium (Cel), while the element that has the lowest grade is Thulium (Tm) with a grade of 0.3 ppm. The graph of the analysis result using the ICP-OES method can be seen in the following figure.

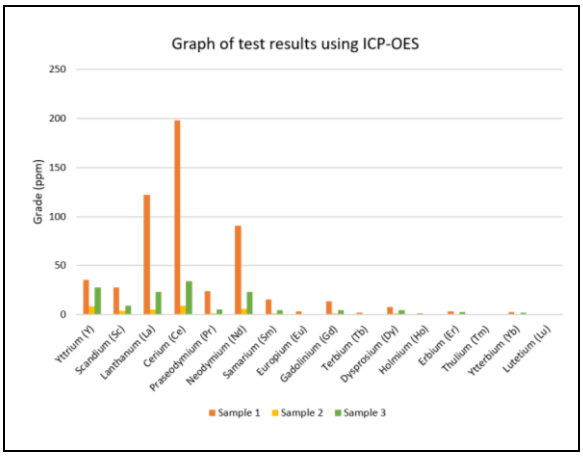

Fig. 8. Rare earth element content in each sample

3.4 Classification of Rare Earth Elements

1. Light rare earth elements

The light rare earth elements consist of Lanthanum (La), Cerium (Ce), Praseodymium (Pr), Neodymium (Nd), and Samarium (Sm). Light rare earth elements have atomic numbers 63 and below. Based on Table 1, it can be seen that the light rare earth element Lanthanum (La) contains grades ranging from 5.3-122 ppm, the Cerium (Ce) element contains grades ranging from 9.4-198 ppm, the Praseodymium (Pr) element contains grades ranging from 1.3-23.6 ppm, the Neodymium (Nd) element contains grades with a range between 6-90.9 ppm and the Samarium (Sm) element contains grades with a range between 1.2-15.4 ppm.

2. Heavy rare earth elements

Heavy rare earth elements consist of the remaining light rare earth elements consisting of Yttrium (Y), Europium (Elu), Gadolinium (Gd), Terbium (Tb), Dysprosium (Dy), Holmium (Ho), Erbium (Er), Ytterbium (Yb) and Lutetium (Lu). Heavy rare earth elements have atomic numbers 64-71. Based on table 1, it can be seen that the Yttrium (Y) element contains a range of grades between 8.7-35.5 ppm, the Europium (Elu) element contains a range of grades between 0.6-3.5 ppm, the Gadolinium (Gd) element contains a range of grades between 1.4-13.5 ppm, the Terbium (Tb) element contains a range of grades between 0.24-1.75 ppm, Dysprosium (Dy) elements contain grades ranging from 1.4-7.9 ppm, Holmium (Ho) elements contain grades ranging from 0.3-1.3 ppm, Erbium (Er) elements contain levels ranging from 0.8-3.2 ppm, Ytterbium (Yb) elements contain grades ranging from 0.8-2.4 ppm and finally Lutetium (Lu) elements containing levels ranging from 0.14-0.39 ppm.

4. Discussion

4.1 High Cerium (Ce) Content

Based on the results of ICP-OES analysis, it can be seen that the element Cerium (Ce) has a fairly high content, namely 198 ppm in sample 1, 9.4 ppm in sample 2, and 34.2 ppm in sample 3. This can be caused by several things, including:

1. The Unique Geochemical Properties of Cerium

Cerium (Ce) is the only element in the rare earth element (REE) group that can undergo oxidation from Ce^{3+} to Ce^{4+}. Under oxidative conditions (e.g., in shallow marine environments or other oxidised environments), Ce^{3+} will change to Ce^{4+}, which is less soluble in water. Ce^{4+} tends to precipitate or adsorb more easily onto mineral surfaces, especially manganese oxides (Cabral et al., 2019). As a result, Ce is more easily enriched in manganese deposits than other REEs such as Nd, La, or Sm.

2. Adsorption Capacity of Manganese Oxides

Manganese oxides such as birnessite, vernadite, and romanechite have an excellent structure for absorbing metal ions from solutions. This structure is anionic (negatively charged), making it easy to bind metal cations such as Ce^{4+} (Serrano and Garcia, 1998). Manganese oxide is known to be highly selective and efficient in adsorbing Ce and other REEs, but Ce^{4+} has the highest affinity due to its charge and ion size (Addy, 2022).

3. Supportive Precipitation Environment

Manganese deposits often form in deep sea, lake, or lateritic soil environments with oxidative conditions. These environments can oxidise $Ce^{3+} \rightarrow Ce^{4+}$ dan Providing a manganese oxide mineral surface for adsorption and co-precipitation of Ce^{4+} (Banakar et al., 1994).

4.2 REE-bearing minerals

Rare earth elements are distributed in various types of minerals, including monazite, bastnasite, xenotime, and others. Manganese minerals can also contain rare earth elements (REE), especially in certain deposits such as marine manganese nodules and manganese laterites (Liu et al., 2018). Although not the primary source of REE like bastnaesite or monazite, manganese minerals have the potential to act as carriers of REE, particularly in the form of adsorption or inclusion. Manganese minerals and oxides—especially MnO_2 and hydrated manganese oxides—play a significant role as carriers and absorbers of REE through surface adsorption mechanisms and even oxidation (particularly for Ce) (Ohta & Kawabe, 2001). In other studies, REE content with an average concentration of 509 ppm was found in manganese ore minerals such as rhodochrosite, ropperite, tetalite, and capillitite (Hai et al., 2020). Thus, it can be concluded that rare earth elements in manganese deposits in the study area are found in manganese oxide minerals, namely pyrolusite (MnO_2) and rhodochrosite ($MnCO_3$).

5. Conclusion

The minerals found in manganese samples in the study area are: Albite, Chlorite, Plagioclase, Orthoclase, Quartz, chlorite, Opaque, Pyrolusite, Muscovite, Diopside, Hematite, Rodochrosite, Manganochromite and Manganite. Rare earth elements in the 3 samples studied in the research area contain 16 elements including Yttrium (8.7-35.5 ppm), Scandium (4-28 ppm), Lanthanum (5.3-122 ppm), Cerium (9.4-198 ppm), Praseodymium (1.3-23.6 ppm), Neodymium (690.9), Samarium (1.2-15.4 ppm), Europium (0.6-3.5 ppm), Gadolinium (1.4-13.5 ppm), Terbium (0.241.75 ppm), Dysprosium (1.4-7.9 ppm), Holmium (0.3-1.3 ppm), Erbium (0.8-3.2 ppm), Thulium (0.1-0.4 ppm), Ytterbium (0.8-2.4 ppm) and Lutetium (0.14-0.39 ppm). These results indicate that manganese deposits in Anabanua Village, Barru Regency, have the potential to be a source of LREE (La, Ce, Pr, Nd, and Sm) with concentrations exceeding those of several deposits around the world, making them worthy of consideration in strategic mineral exploration in Indonesia in general.

Acknowledgements

The author would like to thank the Institute for Research and Resource Development (LP2S) Universitas Muslim Indonesia, which has provided financial support for this research.

References

Ahmed M.A., Mirza T. A, & Kalaitzidis, S.P., 2023. Petrography and geochemistry of the Baska Piwaza ore mineralization, Halgurd Mountain, Iraqi Kurdistan Region: Insights on the Genesis. Iraqi Geological Journal, 56 (2B), 114-136. https://doi.org/10.46717/igj.56.2B.9ms-2023-8-18

Addy, SK., 2022. Rare earth element composition of manganese nodules and micronodules from the northwest Atlantic [dataset bundled publication]. PANGAEA, https://doi.org/10.1594/PANGAEA.943839

Ashok D, Harini BP. 2023. Spatial evaluation of the heavy metal iron in soil, pond water and its mobility into the muscles of zebrafish using ICP-OES. Agricultural Science Digest, 44(2): 382–387. DOI: 10.18805/ag.D-5869.

Al-Jubury, H. E., Agha, M. Y. T., & Aqrawi, A. M., 2023. Petrography and Geochemical Relationships of the Ultramafic Rocks in Galalah area within Erbil Governorate, NE Iraq. Iraqi Journal of Science, 228-252. https://doi.org/10.24996/ijs.2023.64.1.23

Ariansyah. M. R, Massinai, M. F. I., & Altin, M., 2020. Rock Types Classification and Distribution on Anabanua Village, Barru Regency, South Sulawesi. Jurnal Geomine, 8(1), 1-8. https://doi.org/10.33536/jg.v8i01.1385

Atwood D.A, 2013. The rare earth elements: fundamentals and applications, 629 p., John Wiley & Sons.

Burton. J, 2022. US Geological Survey releases-2022 list of critical minerals. USGS.

Cabral, A.R., Zeh, A., Vianna, N.C. et al., 2019. Molybdenum-isotope signals and cerium anomalies in Palaeoproterozoic manganese ore survive high-grade metamorphism. Sci Rep 9, 4570. https://doi.org/10.1038/s41598-019-40998-5

Chen K. 2016. Indirect determination of Sulfate in surface water and groundwater by inductively coupled plasma atomic emission spectrometry. Metallurgical Analysis, 36(9): 73–76. (in Chinese) DOI: 10.13228/j.boyuan.issnl000-7571.009892.

Duz, M.Z., Sagirdag, M., Celik, KS., Hasan, M.A., & Kilinc, E., 2016. Geochemical multi-element ICP-OES analysis of borehole waters from SE Anatolia, Atomic Spectroscopy, 37(2), 43-49. https//doi.org/10.46770/AS.2016.02.002

Emsbo, P., McLaughlin, P.I., Breit, G.N., du Bray, E.A., & Koenig, A.E., 2015. Rare earth elements in sedimentary phosphate deposits: solution to the global REE crisis? Journal of Gondwana Research. https://doi.org/10.1016/j.gr.2014.10.008

Farhadiyan S, Kiani A, Noghre N, et al. 2024. Assessment of trace elements in Iranian kefir samples by using ICP-OES

technique. International Journal of Environmental Analytical Chemistry, 0306–7319. DOI: 10.1080/03067319.2024.2359053.

Falah, D., 2009. Eksplorasi Mangan Palludda Desa Pattappa Kecamatan Pujananting Kabupaten Barru. Dinas Pertambangan dan Energi Kabupaten Barru.

Ghobadi, M. H. , Mousavi, S. , Heidari, M. & Rafie, B., 2015. The Prediction of the Tensile Strength of Sandstones from their petrographical properties using regression analysis and artificial neural network. Geopersia, 5(2), 177-187. https://doi.org/10.22059/JGEOPE.2015.56094

Humphries, M., 2011. Rare earth elements: The global supply chain, Specialist in energy policy, Congressional research service.

Ilieva D, A. Surleva, Murariu M, Drochioiu G., & M. M. A. Abdullah., 2018. Evaluation of ICP-OES method for heavy metal and metalloids determination in sterile dump material, Solid State Phenomena.

Jha, A., 2014. Rare Earth Materials: Properties and Applications. CRC Press.

Karlinasari, R., Rahardjo, P.P., & Dajaputra, A., 2023. The Mineral characteristic of tropical residual soil using X-Ray Diffraction (XRD) and Scan Electron Microscopy (SEM). Journal of Advanced Civil and Environmental Engineering, 6(1), 42-56. https://doi.org/10.30659/jacee.6.1.42-56

Kupolati, D., Amosun, J., Olayanju, G., Oyebamiji, A., & Fagbemigun T., 2020. Geophysical and Petrographical Study of Apatapiti Charnockitic Rock, Akure, Southwestern Nigeria. Iraqi Journal of Science, 1328-1344. https://doi.org/10.24996/ijs.2020.61.6.11

Liu BB, Han M, Liu J, et al. 2022. Determination of total Sulfur in geothermal water by inductively coupled plasma-atomic emission spectrometry. Journal of Groundwater Science and Engineering, 10(3): 285−291. DOI: 10.19637/j.cnki.2305-7068.2022.03.006.

Liu H, Pourret O, Guo H, Martinez RE, & Zouhri L., 2018. Impact of Hydrous Manganese and Ferric Oxides on the Behavior of Aqueous Rare Earth Elements (REE): Evidence from a Modeling Approach and Implication for the Sink of REE. International Journal of Environmental Research and Public Health. 15(12):2837. https://doi.org/10.3390/ijerph15122837

Moriyama. T, Panigrahi, M. K., Pandit, D., & Watanabe, Y., 2008. Rare earth element enrichment in Late Archean manganese deposits from the Iron Ore Group, East India. Resource geology, 58(4), 402-413. https://doi.org/10.1111/j.1751-3928.2008.00072.x

Mustafa, T.A., Mirza, T.A., & Kalaitzidis, S.P., 2023. Petrographical and geochemical features of sulfide mineralization in the Walash Group, Gallala Area, Kurdistan Region of Iraq. Iraqi Geological Journal, 56(2E), 19-36. https://doi.org/10.46717/igj.56.2E.2ms-2023-11-7

Ohta, A., & Kawabe, I., 2001. REE (III) adsorption onto Mn dioxide (δ-MnO2) and Fe oxyhydroxide: Ce (III) oxidation by δ-MnO2. Geochimica et Cosmochimica Acta, 65(5), 695-703. https://doi.org/10.1016/S0016-7037(00)00578-0

Purawiardi, R., 2001. Endapan Unsur-unsur Tanah Jarang dan Batuan Granit, Majalah Metalurgi Volume 16 Nomor 1, Juni 2001, LIPI, Serpong.

Qiao YY, Zhang XW, Fu YG. 2022. Determination of trace elements in drinking water samples by atomic spectroscopy. Modern Food, 28(1): 142−144. (in Chinese) DOI: 10.16736/j.cnki.cn41-1434/ts.2022.01.040.

Ranjbaran, M., Javanmard, S.R., & Sotohian, F., 2019. Petrography and Geochemistry of Quaternary travertines in the Ab-Ask region, Mazandaran Province-Iran. Geopersia, 9(2), 351-365. https://doi.org/10.22059/GEOPE.2019.269160.648425

Sasmaz, A., Zagnitko, V. M., & Sasmaz, B., 2020. Major, trace and rare earth element (REE) geochemistry of the Oligocene stratiform manganese oxide-hydroxide deposits in the Nikopol, Ukraine. Ore Geology Reviews, 126, 103772. https://doi.org/10.1016/j.oregeorev.2020.103772

Simandl, G., 2014. Geology and market-dependent significance of rare earth element resources Mineral. Deposita, 49: 889–904. https://doi.org/10.1007/s00126-014-0546-z

Sufriadin, Nur. I, & Widodo, S., 2015. Studi Mineralogi dan Geokimia Endapan Mangan Daerah Paluda, Kabupaten Barru, Sulawesi Selatan, Proceeding, seminar nasional kebumian ke-8 academia-industry linkage.

Serrano, J.G., & O.C.D. Garcia, 1998. Ce^{3+} adsorption on hydrated MnO_2 . J Radioanal Nucl Chem 230, 33–37. https://doi.org/10.1007/BF02387443

Voica C, M.H. Kovacs, Dehelean A, Ristoiu D, & A. M. Iordache., 2012. ICP-MS determinations of heavy metalsin surface waters from Transylvania, Romanian Journal of Physics, 57(7-8), 1184-1193.

XU Hai, GAO Junbo, YANG Ruidong, DU Lijuan, LIU Zhichen, CHEN Jun, FENG Kangning, YANG Guanghai., 2020. Genesis for Rare Earth Elements Enrichment in the Permian Manganese Deposits in Zunyi, Guizhou Province, SW China[J]. Acta Geologica Sinica,94(1):90-102. https://doi.org/10.1111/1755-6724.14338

Yazdi, P., Kananian, A., Raeisi, D., & Modabberi, S., 2023. Geochemistry, petrogenesis and petrology of intrusive rocks in Shadan gold deposit, SW Birjand, Eastern Iran. Geopersia, 13(1), 33-48. https://doi.org/10.22059/GEOPE.2022.347096.648668

Y. K. Banakar, & P. Jauhari., 1994.Geochemical Trends in the Sediments and Manganese Nodules from a Part of the Central Indian Basin. Jour. Geol. Soc. India., 43 (5): 591–598. doi: https://doi.org/10.17491/jgsi/1994/430510

Zou J, Yang Q, Luo W, et al. 2017. Determination of Sulfur and Boron in salt lake brine and salt products using inductively coupled plasma atomic emission spectrometry. Fine Chemical Intermediates, 47(1): 63−65. (in Chinese) DOI: 10.19342/j.cnki.issn.1009-9212.2017.01.017.